Cell Reports, Volume *16*

Supplemental Information

Synthetic Biology Platform for Sensing and Integrating Endogenous Transcriptional Inputs in Mammalian Cells

Bartolomeo Angelici, Erik Mailand, Benjamin Haefliger, and Yaakov Benenson

Supplemental Figure Titles and Legends

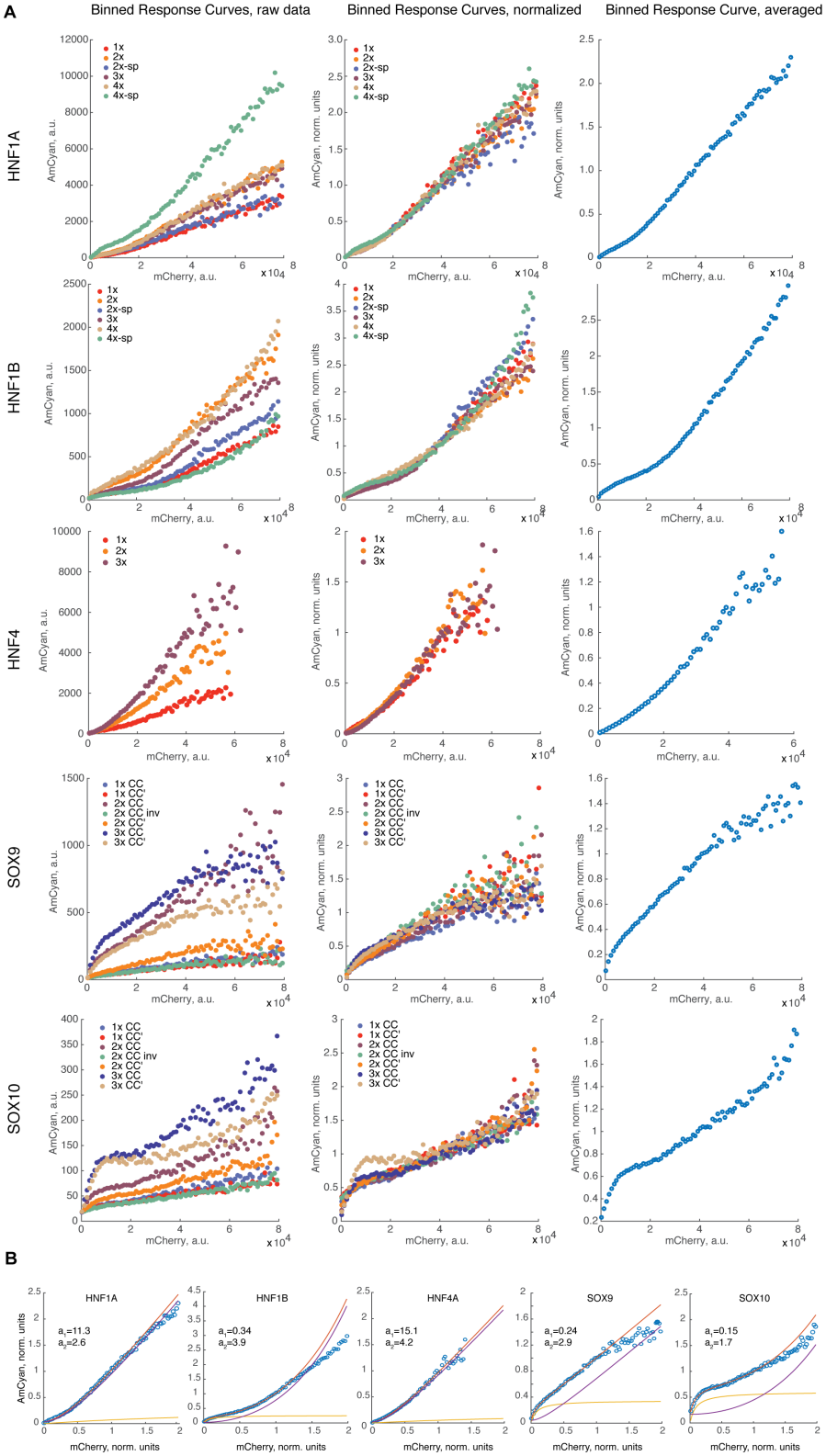

Figure S1. Related to Figure 1. (**A**) Fine binning of the response curves of open-loop TF sensors. Left to right, individual REs' response curves; curves normalized to output expression in the 40th bin (40,000 arbitrary flow cytometry units); averaged normalized curve. Transcription factors and individual response elements are indicated. (**B**) Deconvolution of

the open-loop response curves into a quadratic-linear (purple curve) and a saturating response (brown curve). The sum of the responses is a red curve. The fitted parameters of the saturating component are shown (a_1, the "IC50"; a_2, saturation level, in arbitrary units)

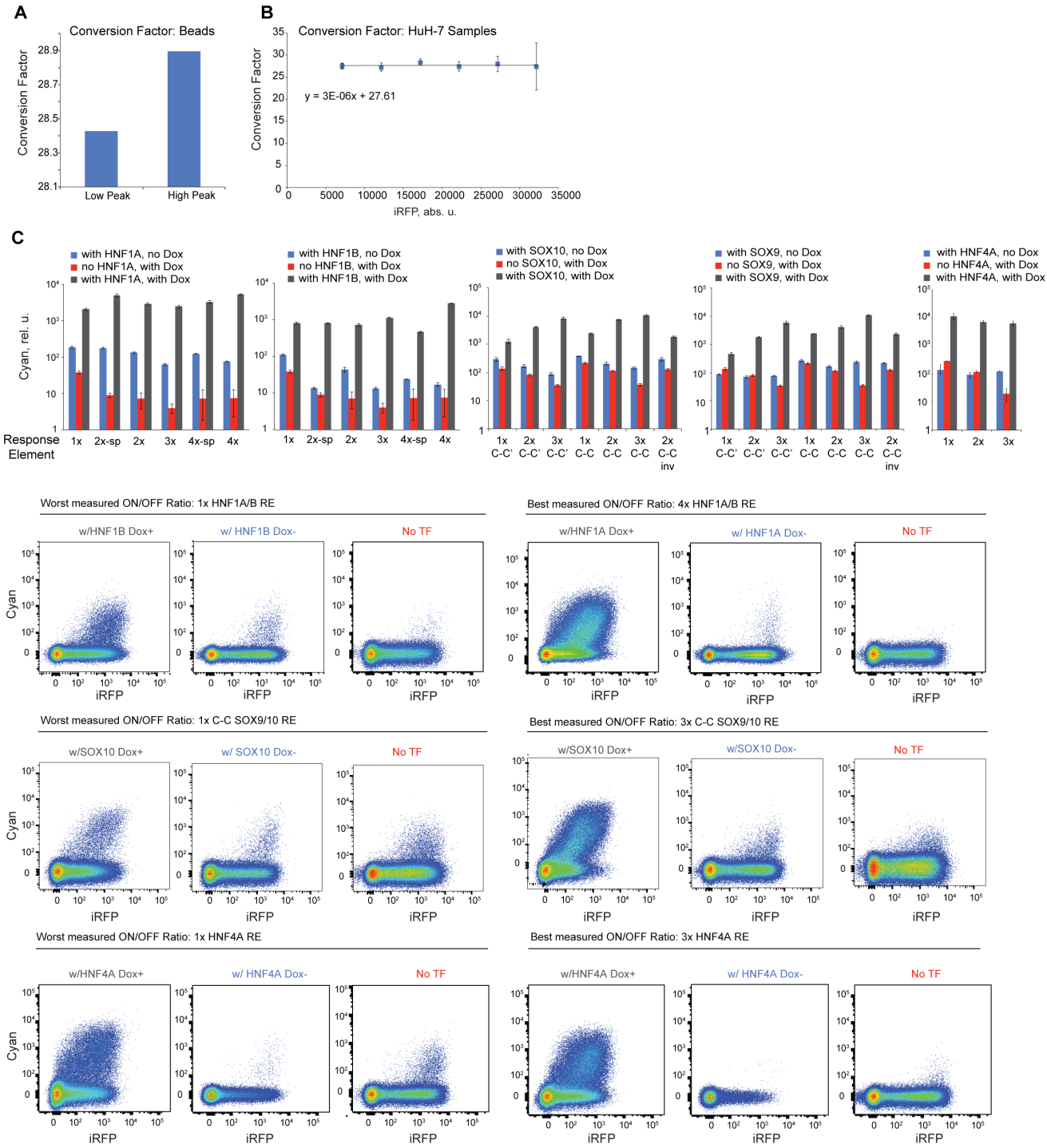

Figure S2. Related to Figure 2. **(A,B)** Calculating the conversion factor between different flow cytometer settings for comparing open-loop and feedback sensors. **(A)** Conversion factor calculated using SPHERO RainBow Calibration particles measured with photomultiplier voltages of 250V and 400V, respectively, and filter settings corresponding to AmCyan readout. The bars show the ratio between fluorescence units measured using the two settings. **(B)** The conversion factor calculated using the same samples measured with different PMT voltages. The dots and the linear regression show the conversion factor (AmCyan at PMT voltage of 400V/AmCyan at PMT voltage of 250V) as a function of iRFP transfection control intensity (measured using constant PMT settings), error bars represents s.d. of three biological replicates. **(C)** The feedback-amplified outputs in HEK293 Tet-On cells in the presence of ectopic TFs compared to the background expression without Dox (but with the ectopic cassette) and the background measured in the absence of TF-encoding gene. The bar charts summarize the data for all the response elements for the five transcription factors. Each bar represents mean±s.d. of three biological replicates. Below, flow cytometry plots show the best and the worst cases for each Transcription Factor family.

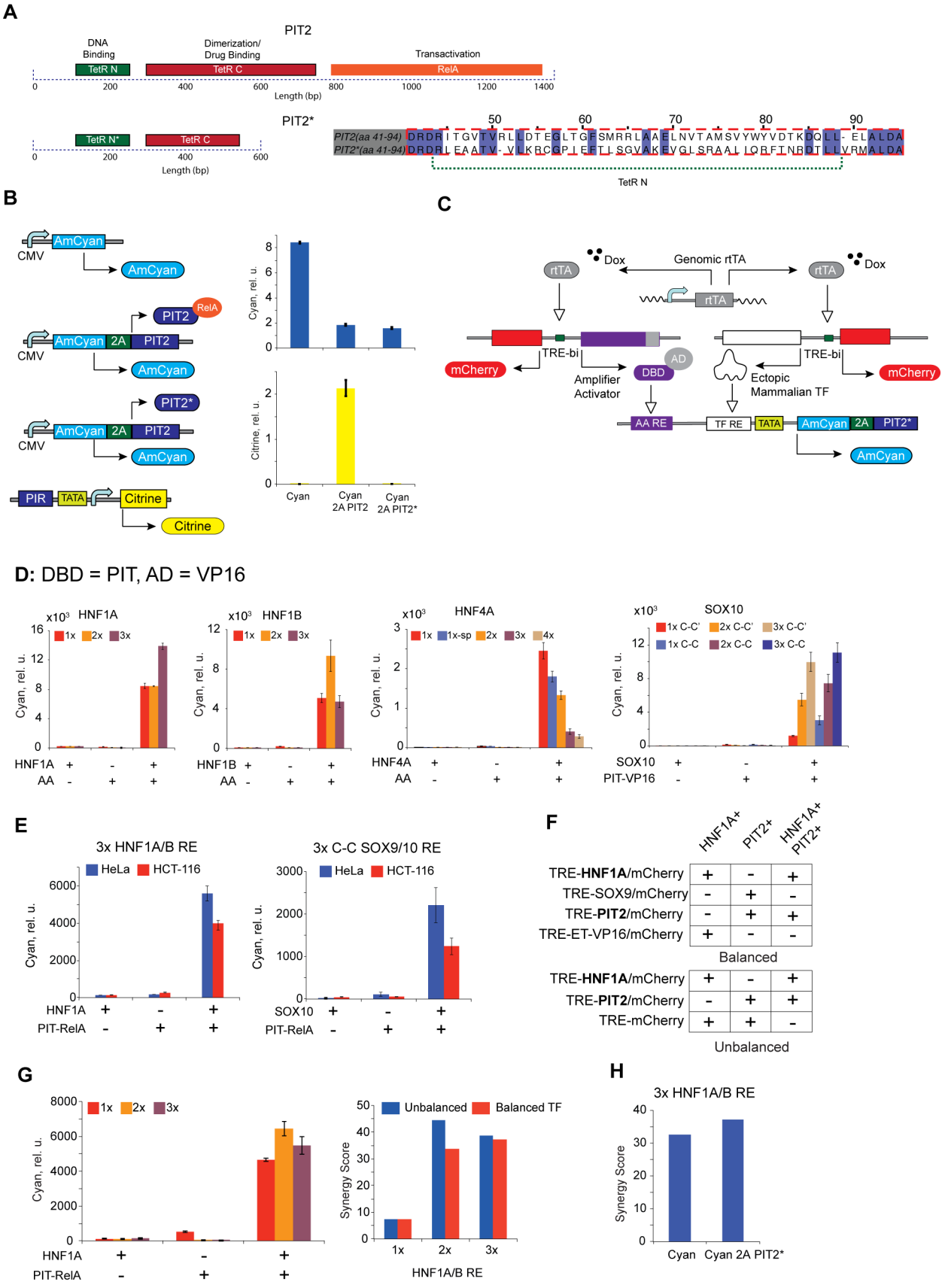

Figure S3. Related to Figure 3. (**A,B**) Evaluation of PIT2 loss-of-function mutant and the effect of 2A linker on gene expression. (**A**) Schematics of mutation in the PIT2 gene. We swap the DNA binding domain with the one derived from the ET transcriptional regulator, and preserve the rest of the sequence in order to enable direct comparison to the readouts

of feedback circuits. The resulting mutant protein PIT2* has high sequence homology with the original PIT2 but is unable to bind DNA due to the mismatch between its binding and dimerization domains. We also delete the transactivation domain. (**B**) Funcitonal evaluation of PIT2 mutant. Left, constructs used in the experiment. Various AmCyan-driving constructs (not coupled to PIT2, coupled to PIT2 via 2A linker, and coupled to PIT2 mutant via 2A linker) are contransfectd with the PIR-Citrine reporter. Only the AmCyan-2A-PIT2 is able to transactivate the reporter. Note that the AmCyan intensity drops 5-fold due to the 2A linker introduction. Each bar represents mean±s.d. of three biological replicates. (**C-H**) Data related to synergy measurements (**C**) Detailed schematics of the synergy measurements. Both the TF of interest and the amplifier activators are controlled via TRE promoters, and each is coexpressed with mCherry reporter. For partial activation conditions (TF only or AA only), the omitted activator is replaced with a similar construct expressing mCherry and a "balancing" factor that does not bind to the composite promoter. (**D**) The effect of replacing the transactivation domain of the amplifying activator from RelA to VP16. Top, different transcriptional complexes are shown. The bar charts' layout is similar to that in Figure 3 C. Each bar represents mean±s.d. of three biological replicates. (**E**) Synergy measurements in two additional cell lines, HeLa and HCT-116. The response elements and TF inputs are indicated. CMV-rtTA was transfected into the cell lines to enable Dox-controleld induction of TRE-TF and TRE-AA constructs. Each bar represents mean±s.d. of three biological replicates. (**F**) Plasmid mixtures used to produce the different combinations of transcriptional inputs for the Balanced and the Unbalanced cases. Shorthand notations of the constructs are indicated, with TRE-X/Y meaning a bidirectional TRE promoter expressing genes X and Y. (**G**) Synergy measurements for the Unbalanced setup. Left, expression levels reached with either, or both, transcriptional inputs provided to the composite promoters containing HNF1A response elements in the Unbalanced transfection setup. Each bar represents mean±s.d. of three biological replicates. Right, comparison of the synergy scores of the same composite promotersin the Balanced and Unbalanced setups. (**H**) Comparison of the measured synergy scores between two HNF1A/B composite promoter driving, respectively, the expression of the Cyan fluorescent protein alone or the mutated feedback loop (Cyan 2A PIT2*). We use PIR::3x-HNF1A/B RE composite promoter because it has the highest synergy in the original dataset.

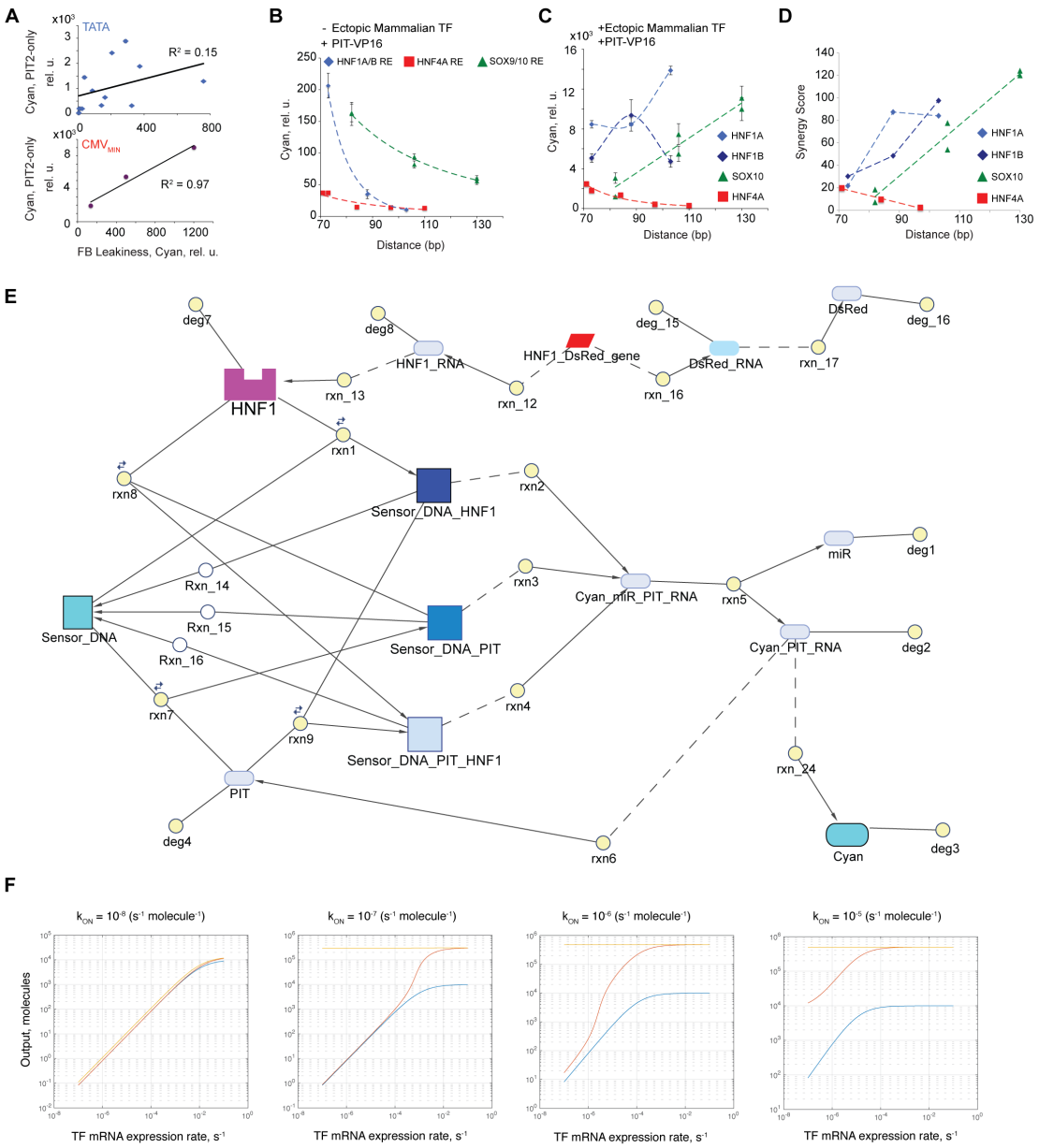

Figure S4. Related to Figure 4. (**A**) The relationship between the intrinsic sensor leakiness as measured with feedback-amplified sensors in the absence of the input TF, and the transactivation efficiency of the amplifier activator alone. Top, all sensors that employ minimal TATA box; bottom, sensors employing CMV_{MIN}. (**B**) Transactivating efficiency of PIT-VP16 amplifier activator alone, as a function of PIR distance from the TATA box. Error bars represent s.d. of three biological replicates (**C**) Fully induced expression levels from a composite promoter achieved by providing both the indicated ectopic TF input and the amplifier activator PIT-VP16 (synergized expression). Error bars represent s.d. of three biological replicates. (**D**) Synergy scores for different composite promoters with PIT-VP16 as amplifier activator as a function of PIR distance from the TATA box. (**E**) The model created in SimBiology to simulate the synergistic amplified loop. (**F**) Simulation results showing the outputs of the open loop, synergistic amplified loop, and an amplified loop without synergy as a function of TF expression rate. The charts are simulated for different values of TF binding rate constant K_{ON} as indicated.

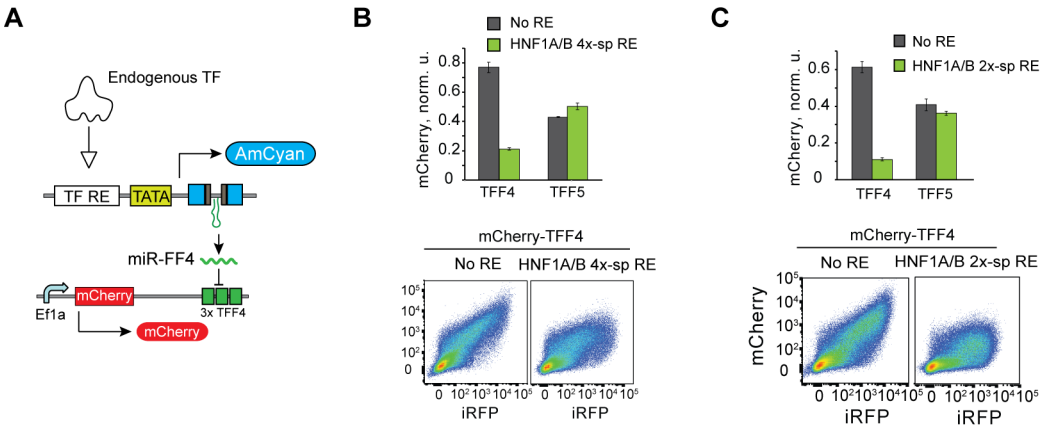

Figure S5. Related to Fig. 7. (**A**) The schematics of TF-induced RNAi. (**B**) Bulk effects and representative flow cytometry plots of mCherry fluorescence in the absence and the presence of a sensor in HuH-7 cells. TFF4 and TFF5 indicate constitutive mCherry constructs fused with these targets. TFF5 is not targeted by miR-FF4. (**C**) RNAi induced by the amplified HNF1A/B 2x-sp RE sensor in HuH-7 cells. Bulk comparison is at the top with representative flow cytometry scatter plots shown below. iRFP serves as a transfection marker. In panels **B** and **C** each bar represents mean±s.d. of three biological replicates

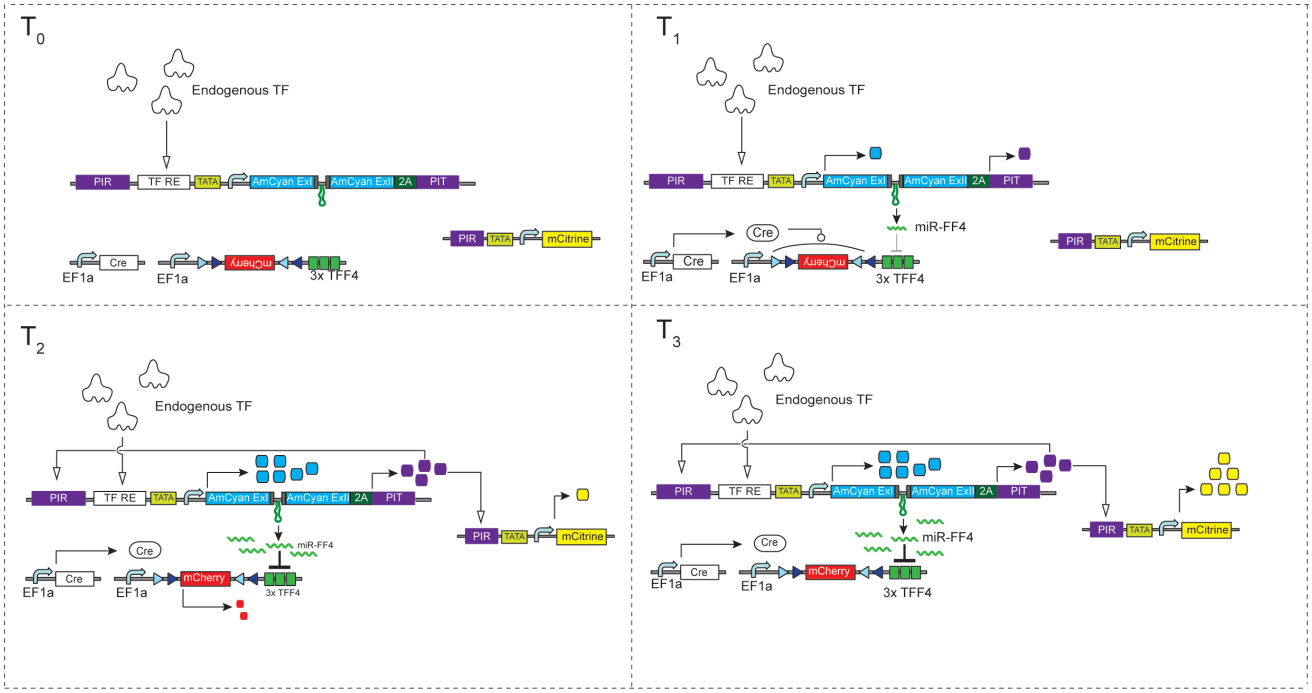

Figure S6. Related to Fig. 7. Schematic representation of the multipronged actuation circuit dynamics. The continuous process is broken down in four separate phases for clarity. In each phase the number of colored boxes is a visual representation of the relative protein concentration and the presence of arrows indicates reactions taking place at a meaningful rate in the specific phase: transcriptional regulation at the promoter level (open arrows), translation or post-transcriptional modifications (solid arrows) and DNA inversion (circular arrowhead).

Supplemental Tables

Table S1. Related to Figure 2. Quantitative outputs with feedback-amplified sensors and the background expression. The values are factored to be directly comparable with open-loop values.

Ectopic TF	Sensor	+TF/+Dox	+TF/-Dox	-TF/+Dox	On/Off Ratio
HNF1A	1x	2053.13	184.39	38.03	54
	2x-sp	4948.82	177.22	8.97	552
	2x	2885.65	132.87	7.13	405
	3x	2440.62	62.94	3.98	613
	4x-sp	3248.16	122.53	7.29	446
	4x	5198.07	75.00	7.44	699
HNF1B	1x	803.61	111.25	38.03	21
	2x-sp	813.16	13.65	8.97	91
	2x	727.66	43.38	7.13	102
	3x	1141.45	13.37	3.98	287
	4x-sp	467.25	23.92	7.29	64
	4x	2820.24	16.95	7.44	379
SOX9	1x C-C’	1234.81	287.41	134.65	9
	2x C-C’	4029.96	162.72	80.75	50
	3x C-C’	8222.87	86.22	34.59	238
	1x C-C	2343.46	373.45	211.67	11
	2x C-C	7290.15	205.02	113.95	64
	3x C-C	10600.37	141.50	36.14	293
	2x C-C inv	1758.33	287.18	123.26	14
SOX10	1x C-C’	465.67	87.75	134.65	3
	2x C-C’	1787.43	70.08	80.75	22
	3x C-C’	5819.88	77.63	34.59	168
	1x C-C	2369.78	267.77	211.67	11
	2x C-C	4146.43	164.64	113.95	36
	3x C-C	10729.40	239.97	36.14	297
	2x C-C inv	2300.66	218.45	123.26	19
HNF4A	1x	11398.15	136.26	283.59	40
	2x	7188.26	92.91	119.68	60
	3x	6319.61	122.29	19.94	317

Table S2. Related to Figure 5. Quantitative outputs with feedback-amplified sensors and corresponding background expression. The specific conditions of induction for each TF are described above in **Forward design of amplified sensors**. The values are factored to be directly comparable with open-loop values.

TF	Sensor	Induced	Non Induced	On/Off Ratio
HIF1A	1x	12910.06	352.51	16
	2x	7644.67	247.50	29
	3x	9168.04	140.15	48
TCF/LEF	1x	3233.7	20.3	159
	3x	7629.3	41.3	185
	6x	3950.4	29.1	136
CA-NFATC1	1x	12910.06	76.60	169
	2x	7644.67	42.70	179
	3x	9168.04	29.54	310

Table S3. Related to Material and Methods. Oligonucleotide and gBlock sequences used for cloning.

Primer name	Sequence 5' → 3'
PR0121	CGCGCCAGTTAATAATTAACTTAGCGCCGGCAGTTAATAATTAACTTCCATATGCTCTAG AGGGTATATAATGGGGGCCA
PR0122	CTAGTGGCCCCCATTATATACCCTCTAGAGCATATGGAAGTTAATTATTAACT GCCGGCGCTAAGTTAATTATTAACTGG
PR0123	CGCGCCAGTTAATAATTAACTTAGCGCCGGCAGTTAATAATTAACTTAGCGCCGGCAGTT AATAATTAACTTAGCGCCGGCAGTTAATAATTAACTCA
PR0124	TATGAGTTAATTATTAACTGCCGGCGCTAAGTTAATTATTAACTGCCGGCGCTAAGTTAA TTATTAACTGCCGGCGCTAAGTTAATTATTAACTGG
PR0125	TCAATTACTAGTCTACTACCAGAGCTCATCGCTAG
PR0126	CTATTGGCGCGCCCCCGTAGCTTGGCGTAATCA
PR0604	CGCGCCAGTTAATAATTAACTAGTTAATAATTAACTCA
PR0605	TATGAGTTAATTATTAACTAGTTAATTATTAACTGG
PR0606	CGCGCCAGTTAATAATTAACTAGTTAATAATTAACTAGTTAATAATTAACTCA
PR0607	TATGAGTTAATTATTAACTAGTTAATTATTAACTAGTTAATTATTAACTGG
BA 1.68.3	CGCGCCAGTTAATAATTAACTAGTTAATAATTAACTAGTTAATAATTAACTAGTTAATAA TTAACTCA
BA 1.68.4	TATGAGTTAATTATTAACTAGTTAATTATTAACTAGTTAATTATTAACTAGTTAATTATTA ACTGG
PR0387	CTCTACAGATCTATGAGTCGAGGAGAGGTGCG
PR0388	GAGAGTAAGCTTTCCTTAGGAGCTGATCTGACTCA
PR0421	CATGTGAAATAGCGCTGTACAGCGTATGGGAATCTCTTGTACGGTGTACGAGTATCTTCC CGTACACCGTACGG
PR0422	CGCGCCGTACGGTGTACGGGAAGATACTCGTACACCGTACAAGAGATTCCCATACGCTG TACAGCGCTATTTCA
PR0431	CCGGAAGAGCCGAGGGCAGGGGAAGTCTTCTAACATGCGGGGACGTGGAGGAAAATCC CGGGCCCA
PR0432	GATCTGGGCCCGGGATTTTCCTCCACGTCCCCGCATGTTAGAAGACTTCCCCTGCCCTCG GCTCTT
PR0700	CATCCTGCGGCCGCCATTTCCCCGAAAAGTGCCACC
PR0702	CATCCTAAGCTTGCTACTTGTACAGCTCGTCCATGC
PR1012	GCCACGGGCGCGCCGCTAGAGCTCGCGGTGCCGAATTCT
PR1013	GGAGCAGGTACCGTCGACTGCAGAATTCG
PR1402	GCAGCGGCTAGCTCACGACACCTGAAATGGAAGAAAAAAACT
PR1409	GCACCAATTAATGCTCCGGTGCCCGTC
PR1410	GGTACTTCGGCGCGCCGCCACCATGGTGAGCAAGGGC
PR1411	GGTACTTCCTCGAGCTACTTGTACAGCTCGTCCATGCCGC
PR1446	CAACCAAAGAGATTCCTCATAAAAACCAAAGAGATTCCTCATAAAAACCAAAGAGATTC CTCATAAAC
PR1269	CGCGCCGGTTCAAAGTCCACA
PR1270	TATGTGGACTTTGAACCGG
PR1271	CGCGCCGGTTCAAAGTCCAGGTTCAAAGTCCACA
PR1272	TATGTGGACTTTGAACCTGGACTTTGAACCGG
PR1273	CGCGCCGGTTCAAAGTCCAGGTTCAAAGTCCAGGTTCAAAGTCCACA
PR1274	TATGTGGACTTTGAACCTGGACTTTGAACCTGGACTTTGAACCGG
PR1447	CCGGGTTTATGAGGAATCTCTTTGGTTTTTATGAGGAATCTCTTTGGTTTTTATGAGGAAT CTCTTTGGTTGGTAC
PR1796	CGCGCCCTACACAAAGCCCTCTGTGTAAGACA
PR1797	TATGTCTTACACAGAGGGCTTTGTGTAGGG
PR1798	CGCGCCCTACACAAAGCCCTCTGTGTAAGACTACACAAAGCCCTCTGTGTAAGACA
PR1799	TATGTCTTACACAGAGGGCTTTGTGTAGTCTTACACAGAGGGCTTTGTGTAGGG
PR1800	CGCGCCCTACACAAAGCCCTCTGTGTAAGACTACACAAAGCCCTCTGTGTAAGACTACAC AAAGCCCTCTGTGTAAGACA
PR1801	TATGTCTTACACAGAGGGCTTTGTGTAGTCTTACACAGAGGGCTTTGTGTAGTCTTACAC AGAGGGCTTTGTGTAGGG

PR1802	CGCGCCCTACACAAAGCCCTCTTTGTGAGACA
PR1803	TATGTCTCACAAAGAGGGCTTTGTGTAGGG
PR1804	CGCGCCCTACACAAAGCCCTCTTTGTGAGACTACACAAAGCCCTCTTTGTGAGACA
PR1805	TATGTCTCACAAAGAGGGCTTTGTGTAGTCTCACAAAGAGGGCTTTGTGTAGGG
PR1806	CGCGCCCTACACAAAGCCCTTACACAAAGAGACTACACAAAGCCCTTACACAAAGAGAC A
PR1807	TATGTCTCTTTGTGTAAGGGCTTTGTGTAGTCTCTTTGTGTAAGGGCTTTGTGTAGGG
PR1966	CGCGCCGGTTCAAAGTCCAGGTTCAAAGTCCAGGTTCAAAGTCCAGGTTCAAAGTCCAC A
PR1967	TATGTGGACTTTGAACCTGGACTTTGAACCTGGACTTTGAACCTGGACTTTGAACCGG
PR1979	GCACCATCCTAGATCTATGAGTCGAGGAGAGGTGCGCATGG
PR1980	GCACCATCCTCGGCCGAGATGGCGCCGGTCATGTCAGGCGGTGTGCTGGCA
PR2068	CGCGCCCTACACAAAGCCCTCTTTGTGAGACTACACAAAGCCCTCTTTGTGAGACTACAC AAAGCCCTCTTTGTGAGACA
PR2069	TATGTCTCACAAAGAGGGCTTTGTGTAGTCTCACAAAGAGGGCTTTGTGTAGTCTCACAA AGAGGGCTTTGTGTAGGG
PR2206	CGCGCCCGGGTTCAAAGTCCACA
PR2207	TATGTGGACTTTGAACCCGGG
PR2967	CCACTGACCGGTATGGTGCCCAAGAAGAAGAGGAAAG
PR2968	CCACTGGCTCTTCCGGAGTCCCCATCCTCGAGCAGC
PR3094	CGCGCCAGATCAAAGGGGGTACA
PR3095	TATGTACCCCCTTTGATCTGG
PR3096	CGCGCCAGATCAAAGGGGGTAAGATCAAAGGGGGTAAGATCAAAGGGGGTACA
PR3097	TATGTACCCCCTTTGATCTTACCCCCTTTGATCTTACCCCCTTTGATCTGG
PR3098	CGCGCCAGATCAAAGGGGGTAAGATCAAAGGGGGTAAGATCAAAGGGGGTA AGATCAAAGGGGGTAAGATCAAAGGGGGTAAGATCAAAGGGGGTACA
PR3099	TATGTACCCCCTTTGATCTTACCCCCTTTGATCTTACCCCCTTTGATCT TACCCCCTTTGATCTTACCCCCTTTGATCTTACCCCCTTTGATCTGG
PR3104	CGCGCCGGAGGAAAAACTGTTTCATACAGAAGGCGTCA
PR3105	TATGACGCCTTCTGTATGAAACAGTTTTTCCTCCGG
PR3106	CGCGCCGGAGGAAAAACTGTTTCATACAGAAGGCGTGGAGGAAAAACTGTTTCATACAG AAGGCGTCA
PR3107	TATGACGCCTTCTGTATGAAACAGTTTTTCCTCCACGCCTTCTGTATGAAACAGTTTTTCC TCCGG
PR2465	CGCGCCGGAGGAAAAACTGTTTCATACAGAAGGCGTGGAGGAAAAACTGTTTCATACAG AAGGCGTGGAGGAAAAACTGTTTCATACAGAAGGCGTCA
PR2466	TATGACGCCTTCTGTATGAAACAGTTTTTCCTCCACGCCTTCTGTATGAAACAGTTTTTCC TCCACGCCTTCTGTATGAAACAGTTTTTCCTCCGG
PR3217	CGCGCCGACCTTGAGTACGTGCGTCTCTGCACGTATGCA
PR3218	TATGCATACGTGCAGAGACGCACGTACTCAAGGTCGG
PR3219	CGCGCCGACCTTGAGTACGTGCGTCTCTGCACGTATGGACCTTGAGTACGTGCGTCTCTG CACGTATGCA
PR3220	TATGCATACGTGCAGAGACGCACGTACTCAAGGTCCATACGTGCAGAGACGCACGTACT CAAGGTCGG
PR3221	CGCGCCGACCTTGAGTACGTGCGTCTCTGCACGTATGGACCTTGAGTACGTGCGTCTCTG CACGTATGGACCTTGAGTACGTGCGTCTCTGCACGTATGCA
PR3222	TATGCATACGTGCAGAGACGCACGTACTCAAGGTCCATACGTGCAGAGACGCACGTACT CAAGGTCCATACGTGCAGAGACGCACGTACTCAAGGTCGG
PR0761	GCACCAACCGGTCGCCACCATGGTGCCCAAGAAG
PR0763	GCAGCTAAGCTTCTAGAGTCACTAGTTCAGTCCCCATCC
PR0726	CGTGTTTTTCTACAACTGGTTT
PR0727	AGAACTGGACGGGCTGC
PR0504	TATAGAATTCGCCACCATGGTGAGCAAGGGCGAGGAGGATAACAT
PR0550	TATATATCGGCCGCTACTTGTACAGCTCGTCCATGC
PR0534	CAATGCTAGCGCCTCAGACAGTGGTTCAAAG
PR0535	CAGCCACCACCTTCTGATAGG
BA1.68.5	CCTTCATATGTAGGCGTGTACGGTGGGA
BA1.68.7	CCAACCACTAGTGCGATCTGACGGTTCACT

gBlock042	ATGAGTCGAGGAGAGGTGCGCATGGCGAAGGCAGGACGAGAGGGACCACGGGACAGCG TGTGGCTGTCAGGAGAGGGACGGCGCGGCGGTCGCCGTGGAGGACAGCCGTCCGGGCTC GACCGAGACCGGCTCGAGGCCGCCACAGTAGTGCTGAAGCGTTGCGGTCCCATAGAGTT CACGCTCAGCGGAGTAGCAAAGGAGGTGGGGCTCTCCCGCGCAGCGTTAATCCAGCGCT TCACCAACCGCGATACACTGCTGGTGAGGATGGCCCTGGACGCCGTCTTCGGCGAGCTGC GCCACCCAGACCCGGACGCCGGACTCGACTGGCGAGAGGAACTGCGGGCCCTGGCCCGA GAGAACCGGGCACTGCTGGTGCGCCACCCTTGGTCTTCACGGCTGGTCGGCACCTACCTC AACATCGGACCACACTCGCTGGCCTTCTCTCGCGCGGTGCAGAACGTCGTGCGCCGCAGC GGACTGCCAGCACACCGCCTGACA

Table S4. Attached File, Related to Material and Methods. Transfection tables: DNA amounts and plasmid setup used for each experiment. Each Excel sheet is named with a Figure number and panel name and contains the experimental setup to produce the relative panel.

Supplemental Experimental Procedures

Minimal promoter design. In the prototypical core promoter the TATA box is the only AT-rich sequence embedded in a GC rich environment. Several works show the importance of the upstream (BRE^u) and downstream (BRE^d) sequence in modulating transcription initiation. It is well established from *in vitro* experiment that the BRE^u sequence mediates the interaction between the core promoter and the TFIIB core component of the initiation complex (Lagrange et al, 1998). In vitro transcription experiments in mammalian cell-extracts show that as a general trend a reduction in the GC content of the BRE^u reduce the basal level of transcription and the affinity for TFIIB (Wolner & Gralla, 2000).

Based on these observations the upstream sequence of our core promoter was derived from the TATA of E1B Adenovirus (Chen & Manley, 2003) while the rest of the sequence conforms to the classic consensus (Wolner & Gralla, 2000). This BRE^u harbors an imperfect consensus with intermediate GC content and near-background levels of TBP and TFIIB occupancy in vivo that can be increased by transcriptional activation. We call the resulting core promoter TATA Tight (TCTAGAGGGTATATAATGGGGGCCA, yellow shading representing the E1B-derived sequence and the cyan sequence being the consensus). We note that this exact sequence is not found in nature as verified by BLAST.

Response Elements design and promoter architecture. The sequence for the HNF1 response element (AGTTAATAATTTAAC) was derived from the published Positional Weight Matrix using the nucleotides with highest frequency for each position (Tronche et al, 1997a). Despite some differences in the gene activation profile between the two transcription factors (Senkel et al, 2005) the consensus sequence is known to bind both to HNF1A and HNF1B since the two TF share a highly conserved DNA binding domain (Wu et al, 2004).

Response elements in natural promoter often occur with periodic spacing related to DNA phasing (Larsson et al, 2007) and several works tried to test the relation between phasing and transcriptional response in small cis-regulatory modules (Huang et al, 2012). Different minimal promoter architectures were obtained by introducing a variable number of RE in direct tandem repeat or with an intervening 10 bp spacing. The spacer sequence (GCCGCTTAAA) was verified through TRANSFAC DB to confirm the absence of conserved transcription factor binding sites. Since the length of the HNF1 response element is 15 bp, this distance keeps the same DNA helical phasing between the centers of the response element but increase the distance potentially having an influence on the steric interactions.

The sequence for the HNF4A Response Element (GGTTCAAAGTCCA) was chosen over the classic Wild Type based on extensive measurement of DNA binding specificity by protein binding microarrays (Fang et al, 2012) in order to minimize the crosstalk with closely related Nuclear Receptors (RXRa and COUPTF2).

The SOX10 C-C' Response Element (CTACACAAAGCCCTCTGTGTAAGA) differs from the perfect consensus. It is based on the myelin Protein zero (P_0) promoter and is composed of two heptameric elements facing each other and separated by a 4bp spacing (Peirano & Wegner, 2000). The two sites have different affinities for the transcription factor high (C) and low (C') respectively. This arrangement favor dimeric binding improving the specificity for members of SOX group E (SOX8, SOX9 and SOX10) since group E is the only with a conserved dimerization domain (Kuhlbrodt et al, 1998). The SOX10 C-C Response Element (CTACACAAAGCCCTCTTTGTGAGA) is obtained by substituting the low affinity element with a second high affinity site. The resulting sequence was shown to bind SOX10 with higher affinity in vitro.

The sequence for the Hypoxya (HIF1A) Response Element (GACCTTGAGTACGTGCGTCTCTGCACGTATG) was selected based on the PWM derived by Chip-seq experiments (Schodel et al, 2011) and on previous observation suggesting that sequences flanking the minimal HIF1 consensus are important for efficient gene induction (Takagi et al, 1996).

The NFATC1 Response Element (GGAGGAAAAACTGTTTCATACAGAAGGCGT) is derived from the high affinity sequence in the IL-2 promoter (Fiering et al, 1990).

The sequence for the TCF/LEF Response Element (AGATCAAAGGGGGTA) was tested in human cell lines in (Buckley et al, 2015) and based on the previously published Top Flash reporter (Veeman et al, 2003).

Plasmid Construction. Plasmids were constructed using standard cloning techniques. All restriction enzymes used in this work were purchased from New England Biolabs (NEB). Phusion High-Fidelity DNA Polymerase (NEB) was used for fragment amplification. Single-strand oligonucleotides were synthesized by Microsynth or Sigma-Aldrich. Digestion products or PCR fragments were purified using GenElute Gel Extraction Kit or Gen Elute PCR Clean Up Kit (Sigma-Aldrich). Ligations were performed using T4 DNA Ligase (NEB) optimizing temperature, ligation time and molar ratio on a case by case basis. The ligation products were transformed into chemically competent *E.Coli* DH5α that were plated on LB Agar with appropriate antibiotics selection (Ampicillin, 100 µg/ml, Chloramphenicol, 25 µg/ml, Kanamycin, 50 µg/ml). The resulting clones where screened directly by colony-PCR whenever possible (Dream Taq Green PCR Master Mix, Thermo Scientific). We expanded single clones in LB Broth Miller Difco (BD) supplemented with the appropriate

antibiotics and purified their plasmid DNA using GenElute Plasmid Miniprep Kit (Sigma-Aldrich). All the resulting plasmids were verified by Microsynth using Sanger Sequencing. The DNA for mammalian transfection was obtained from 100 ml of liquid culture using the Invitrogen PureLink® HiPure Plasmid Maxiprep Kit (K2100-06). The recovered DNA was further purified using the Norgen Endotoxin Removal Kit Midi (Cat. # 52200) or Maxi (Cat.# 21900). A short cloning procedure for each construct used within this work is described in the Supplemental Information. The transcription factors cDNA used in this study where obtained from the I.M.A.G.E. Consortium library of Human cDNA or produced by RT-PCR in our laboratory (see construct pBA248 below). HNF1A (Clone IRATp970D08125D), HNF1B (clonbe IRATp970A0421D), SOX9 (clone IRATp970C0581D) and SOX10 (clone IRAUp969C0422D) were ordered from SourceBioscience as I.M.A.G.E clones. Primers are listed in Table S2. Specific cloning steps of the constructs employed in this study are as follows:

2x-sp HNF1A/B RE minTATA Cyan F4 (pBA001): pRheo-AmCyan-FF4 Backbone (Leisner et al, 2010) was amplified using primers PR0125 and PR0126 in order to remove the Rheo promoter region and adding AscI and SpeI restriction sites. The resulting product was gel purified, digested and ligated with the annealed oligos PR0121 and PR0122 in order to introduce a 2X Spaced HNF1 response elements flanked by a NdeI restriction site and a downstream minimal TATA Box. The resulting backbone has a modular promoter region that can easily be used to build families of transcriptional reporters or libraries. To obtain reporters with different transcription factors sensitivities pBA001 is digested with AscI and NdeI and ligated with different annealed oligos with matching overhangs. The HNF1 response element is designed according to the PWM described in (Tronche et al, 1997b)

4x-sp HNF1A/B RE minTATA Cyan-F4 (pBA002): PR0123 and PR0124

1x HNF1A/B RE minTATA Cyan-F4 (pBA004): Oligos BA1.68.1 and BA1.68.2

2x HNF1A/B RE minTATA Cyan-F4 (pBA067): Oligos PR0604 and PR0605

3x HNF1A/B RE minTATA Cyan-F4 (pBA068): Oligos PR0606 and PR0607

4x HNF1A/B RE minTATA Cyan-F4 (pBA005): Oligos BA1.68.3 and BA1.68.4

1x HNF1A/B RE CMV_{MIN} Cyan-F4- (pBA006): The CMV_{MIN} promoter was PCR amplified from pTRE-Tight-BI (Clontech Catalog # 631068) using BA1.68.5 and BA1.68.7 primers. The resulting fragment was digested with NdeI and SpeI and cloned in pBA004 linearized using the same restriction enzymes.

CMV Cyan-F4 (pBA008): pBA001 is digested using PciI and NheI to remove completely the promoter region. The CMV promoter is extracted from pAmCyan1-C1 Vector (Clontech #632441) using the same restriction enzymes and cloned in pBA001. The resulting backbone can be used as a strong positive control for response/transduction.

PIR 1x HNF1A/B RE minTATA Cyan F4 (pBA017): Upstream regulatory sequence can be introduced in all the original reporter backbone by digesting with PciI and AscI and ligating annealed oligos with matching overhangs. pBA004 is digested and ligated with annealed PR421 and PR422.

PIR 4x HNF1A/B RE minTATA Cyan F4 (pBA018): pBA005 is digested with PciI and AscI and ligated with PR421 and PR422.

PIR 1x HNF1A/B RE CMV_{MIN} Cyan-F4- (pBA019): pBA006 is digested with PciI and AscI and ligated with PR421 and PR422.

CMV Cyan-F4-PIT2 (pBA012): PIT2 (Pip-p65) was amplified from pMF208 ((Weber et al, 2002)) using PR0387 and PR0388 the resulting product was digested with BglII and HindIII, and cloned into pBA008 digested with the same enzymes to obtain a Cyan-Transactivator fusion protein.

CMV Cyan-F4-2A (pBA022): pBA008 was digested with BspeI and BglII and annealed oligos PR0431 and PR0432 harboring matching overhangs coding for the 2A Viral peptide in order to obtain a bicistronic expression unit.

CMV Cyan-F4-2A-PIT2 (pBA023): PIT2 was extracted from pBA012 with BglII and HindIII and subcolned into pBA022 using the same enzymes resulting in a bicistronic Cyan – Transactivator protein.

PIR 4x HNF1A/B RE minTATA Cyan-F4-2A-PIT2 (pBA028): The coding region (Cyan-F4-2A-PIT2) was extracted from pBA023 cutting with AgeI and HindIII and cloned in pBA018 using the same restriction enzymes.

Similar to pBA001 the resulting backbone can be used as a template for the creation of the different PIT2 feedback amplified transcriptional reporters using the same oligos discussed before. In particular in this study we build and use:

PIR RE 2x-sp HNF1A/B RE minTATA Cyan F4- 2A-PIT2 (pBA141): Oligos BA1.68.3 and BA1.68.4

PIR RE 2x HNF1A/B RE minTATA Cyan F4- 2A-PIT2 (pBA065): Oligos PR604 and PR605

PIR RE 3x HNF1A/B RE minTATA Cyan F4- 2A-PIT2 (pBA066): Oligos PR606 and PR607

PIR RE 4x-sp HNF1A/B RE minTATA Cyan F4- 2A-PIT2 (pBA328): PR0123 and PR0124

PIR RE 1x HNF1A/B RE minTATA Cyan F4- 2A-PIT2 (pBA027): The coding region (Cyan-F4-2A-PIT2) was extracted from pBA023 cutting with AgeI and HindIII and subcloned in pBA017 using the same restriction enzymes.

CMV iRFP (pCS12): Addgene plasmid 31857

pBA142 (HNF1B in pCMVSport6): I.M.A.G.E. Clone IRATp970D08125D

pEM002 (HNF1A in pCMVSport6): I.M.A.G.E. Clone IRATp970A0421D

pEM001 (pTRE-Bi mCherry-HNF1B): Extract HNF1B coding sequence from pBA142 using EcoRI and XbaI and ligate in pIM003 digested using the same restriction enzymes.

pTRE-Bi mCherry-HNF1A (pEM003): The pIM003 was digested with EcoRI,,the resulting overhang was blunted using NEB Quick Blunting Kit (# E1201S) and the resulting linearized backbone was cut with NotI. pEM002 was digested with SpeI, blunted as previously described, and digested again with NotI to extract the HNf1A coding sequence. The two resulting compatible fragments were ligated overnight at 16°C

1x HNF4A RE minTATA Cyan-F4 (pBA160): pBA001 is digested with AscI and NdeI and ligated with annealed oligos (PR1269-PR1270) harboring matching overhangs. The HNF4A specific response element is designed according to the PWM described in (Fang et al, 2012). In this study we similarly construct and use:

2x HNF4A RE minTATA Cyan-F4 (pBA161): Oligos PR1271-PR1272

3x HNF4A RE minTATA Cyan-F4 (pBA162): Oligos PR1273-PR1274

Pir 1x HNF4A RE minTATA Cyan-F4-2A-PIT2 (pBA163): A HNF1 Feedback Loop backbone (pBA141) was digested with AscI and NdeI and ligated with annealed oligos (PR1269-PR1270) harboring matching overhangs. In this study we similarly construct and use:

PIR 2x HNF4A RE minTATA Cyan-F4-2A-PIT2 (pBA163): Oligos PR1271-PR1272

PIR 3x HNF4A RE minTATA Cyan-F4-2A-PIT2 (pBA163): Oligos PR1273-PR1274

1x SOX9/10 C-C' RE minTATA Cyan-F4 (pBA342): pBA001 was digested with AscI and NdeI and ligated with annealed oligos (PR1796-PR1797) harboring matching overhangs. The SOX response element is designed according to (Peirano & Wegner, 2000). In this study we similarly construct and use:

2x SOX9/10 C-C' RE minTATA Cyan-F4 (pBA343): Oligos PR1798-PR1799

3x SOX9/10 C-C' RE minTATA Cyan-F4 (pBA344): Oligos PR1800-PR1801

1x SOX9/10 C-C RE minTATA Cyan-F4 (pBA345): Oligos PR1802-PR1803

2x SOX9/10 C-C RE minTATA Cyan-F4 (pBA346): Oligos PR1804-PR1805

2x SOX9/10 C-C_{INV} RE minTATA Cyan-F4 (pBA347): Oligos PR1806-PR1807

3x SOX9/10 C-C RE minTATA Cyan-F4 (pBA489): Oligos PR2068-PR2069

PIR 1x SOX9/10 C-C' RE minTATA Cyan-F4-2A-PIT2 (pBA367): A HNF1 Feedback Loop backbone (pBA141) was digested with AscI and NdeI and ligated with annealed oligos (PR1796-PR1797) harboring matching overhangs. In this study we similarly construct and use:

PIR 2x SOX9/10 C-C' RE minTATA Cyan-F4-2A-PIT2 (pBA368): Oligos PR1798-PR1799

PIR 3x SOX9/10 C-C' RE minTATA Cyan-F4-2A-PIT2 (pBA369): Oligos PR1800-PR1801

PIR 1x SOX9/10 C-C RE minTATA Cyan-F4-2A-PIT2 (pBA370): Oligos PR1802-PR1803

PIR 2x SOX9/10 C-C RE minTATA Cyan-F4-2A-PIT2 (pBA371): Oligos PR1804-PR1805

PIR 2x SOX9/10 C-C_{INV} RE minTATA Cyan-F4-2A-PIT2 (pBA372): Oligos PR1806-PR1807

PIR 3x SOX9/10 C-C RE minTATA Cyan-F4-2A-PIT2 (pBA477): Oligos PR2068-PR2069

pTRE Bidirectional mCherry-HNF4A (pBA266): pBA248 was digested with AgeI and PsPOMI and the resulting HNF4A coding region was cloned in the pIM003 backbone digested using the same restriction sites.

pTRE Bidirectional mCherry-SOX10 (pBA417): pBA402 was digested with XhoI, the resulting overhang was blunted using NEB Quick Blunting Kit (# E1201S). The linearized backbone was further digested with EcoRI, and the extracted TF band was cloned in pIM003 backbone in turn digested with NdeI, blunted as described above, and successively with EcoRI-HF.

pTRE Bidirectional mCherry-PIT2 (pBA427): PIT2 sequence was extracted from pMF206 by EcoRI and BamHI digestion. The sequence was cloned into pIM003 linearized using EcoRI and BamHI

pTRE Bidirectional mCherry-PITVP16 (pBA481): PITVP16 sequence was extracted from pMF156 by EcoRI and BamHI digestion. The sequence was cloned into pIM003 linearized using EcoRI and BamHI.

EF1A mCherry 3X FF3t 3XFF4t (pBA097): pKH026 was PCR amplified using the primers PR0700 and PR0702 adding the NotI and HindIII restriction sites and cloned in EF1a-ZsYellow-FF3x3-FF4x3 (Leisner et al, 2010).

EF1A mCherry 3X FF3t 3XFF4t (pBA098): pKH026 was PCR amplified using the primers PR0700 and PR0702 adding the NotI and HindIII restriction sites and cloned in EF1a-ZsYellow-FF5x3-FF6x3 (Leisner et al, 2010).

Cagop lox2272-loxP-mCherry$_{Inv}$- lox2272-loxP 3XFF4t (pBA221): The LoxP recombination sequence were amplified from pEL097(citation) with PR1012 and PR1013 adding AscI and KpnI restriction sites. mCherry was amplified from pKH026 using PR1410 and PR1411 introducing terminal XhoI and AscI restriction sites. pNL67 (citation) was digested with XhoI and KpnI. All the components were gel purified and a 3-Way Ligation was carried out overnight at 4°C.

EF1A lox2272-loxP-mCherry$_{Inv}$- lox2272-loxP 3XFF4t (pBA224): EF1A promoter was amplified from pKH026 adding using PR1402 and PR1409, the resulting product was digested with AseI and NheI. The promoter was cloned in the pBA221 backbone digested with the same restriction sites.

EF1A lox2272-mCherry- loxP 3XFF4t (pBA225): pBA225 was obtained starting from pBA224 by in vitro recombination using NEB Cre Recombinase (#M0298S), following the suggested protocol.

EF1A lox2272-loxP-mCherry$_{Inv}$- lox2272-loxP 3XFF6t (pBA235): pBA224 was digested with KpnI and XmaI. The resulting product was gel purified and ligated with the annealed oligos PR1446 and PR1447 harboring 3x FF6t flanked by matching overhangs.

EF1A lox2272-mCherry- loxP 3XFF6t (pBA237): pBA224 was digested with KpnI and XmaI. The resulting product was gel purified and ligated with the annealed oligos PR1446 and PR1447 harboring 3x FF6t flanked by matching overhangs.

PIR RE 2x HNF1A/B RE minTATA Cyan F4- 2A-PIT* (pBA435): gBlock042 encoding a mutated version of PIT2 was amplified using PR1979 and PR1980. The product was digested with BglII and EagI and cloned in pBA065 digested with the same restriction enzymes.

pCMV – HNF4A (pBA248): HNF4A cDNA was obtained by extracting the mRNA from HuH-7 cell line using the mirVana miRNA Isolation Kit (Life Techonologies) according to the protocol for Total RNA isolation. The resulting pool was retro-transcribed with the Maxima H Minus First Strand cDNA Synthesis Kit (Thermo Scientific) using the specific primers pair described in (Takagi et al, 2010) and according to the suggested RT conditions. The resulting double stranded DNA was amplified with PR1516 and PR1518 and cloned in pBA008 digested with the same pair of enzymes to produce a constitutive ectopic version of HNF4A

PIR RE 1x HNF1A/B RE minTATA Cyan F4- 2A-PIT* (pBA436): gBlock042 encoding a mutated version of PIT2 was amplified using PR1979 and PR1980. The product was digested with BglII and EagI and cloned in pBA027 digested with the same restriction enzymes.

PIR RE 3x HNF1A/B RE minTATA Cyan F4- 2A-PIT* (pBA437): gBlock042 encoding a mutated version of PIT2 was amplified using PR1979 and PR1980. The product was digested with BglII and EagI and cloned in pBA066 digested with the same restriction enzymes.

PIR RE 1x HNF4A RE minTATA Cyan F4- 2A-PIT* (pBA478): pBA435 was digested with AscI and NdeI and ligated with annealed oligos (PR1269-PR1270) harboring matching overhangs. Using the same strategy we construct also:

PIR RE 3x HNF4A RE minTATA Cyan F4- 2A-PIT* (pBA479): Oligos PR1273-PR1274

PIR RE 2x HNF4A RE minTATA Cyan F4- 2A-PIT* (pBA507): Oligos PR1271-PR1272

PIR RE 4x HNF4A RE minTATA Cyan F4- 2A-PIT* (pBA508): Oligos PR1966-PR1967

PIR RE 1X+2sp HNF4A RE minTATA Cyan F4- 2A-PIT* (pBA509): Oligos PR2206-PR2207

Pir 3x SOX9/10 C-C RE minTATA Cyan-F4-2A-PIT* (pBA480): pBA435 was digested with AscI and NdeI and ligated with annealed oligos (Oligos PR2068-PR2069) harboring matching overhangs. Using the same strategy we construct also:

PIR RE 1x SOX9/10 C-C' RE minTATA Cyan F4- 2A-PIT* (pBA512): Oligos PR1796-PR1797

PIR RE 1x SOX9/10 C-C RE minTATA Cyan F4- 2A-PIT* (pBA513): Oligos PR1802-PR1803

PIR RE 2x SOX9/10 C-C' RE minTATA Cyan F4- 2A-PIT* (pBA514): Oligos PR1798-PR1799

PIR RE 2x SOX9/10 C-C RE minTATA Cyan F4- 2A-PIT* (pBA515): Oligos PR1804-PR1805

PIR RE 3x SOX9/10 C-C' RE minTATA Cyan F4- 2A-PIT* (pBA516): Oligos PR1800-PR1801

PIR 1x HNF1A/B RE CMV_{MIN} Cyan-F4-2A-PIT* (pBA492): Cyan-2A-PIT* is extracted from pBA435 by digestion with AgeI and HindIII. The sequence is cloned in pBA019 backbone digested with the same enzymes

PIR 2x HNF1A/B RE CMV_{MIN} Cyan-F4-2A-PIT* (pBH289): pBA492 is digested with AscI and NdeI and ligated with annealed oligos PR0604 – PR0605

PIR 3x HNF1A/B RE CMV_{MIN} Cyan-F4-2A-PIT* (pBH290): pBA492 is digested with AscI and NdeI and ligated with annealed oligos PR0606 – PR0607

PIR 1x HNF1A/B RE CMV_{MIN} Cyan-F4-2A-PIT2 (pBA493): The Cyan-2A-PIT2 is extracted from pBA165 by digestion with AgeI and HindIII. The sequence is cloned in pBA019 backbone digested with the same enzymes.

PIR 2x HNF1A/B RE CMV_{MIN} Cyan-F4-2A-PIT2 (pBH291): pBA493 is digested with AscI and NdeI and ligated with annealed oligos PR0604 – PR0605

PIR 3x HNF1A/B RE CMV_{MIN} Cyan-F4-2A-PIT2 (pBH292): pBA493 is digested with AscI and NdeI and ligated with annealed oligos PR0606 – PR0607

CMV Cyan-F4-2A-PIT2 (pBA528): The Cyan-2A-PIT2 is extracted from pBA435 by digestion with AgeI and HindIII. The sequence is cloned in pBA019 backbone digested with the same enzymes.

pEL0172 Pir 30bp Spacer mCitrine (pEL0172): As described (Prochazka et al, 2014).

Ef1A iCRE (pNL108): As described (Lapique & Benenson, 2014).

Ef1α-mCherry (pKH026): mCherry was PCR amplified from Addgene plasmid 30125 (pKH015) using primers PR0504 and PR0550 and cloned into Addgene plasmid 11154 (pKH013) after digestion with EcoRI and EagI

pTRE Bidirectional mCherry-pA (pIM003): mCherry was amplified from pKH0026 with primers PR0534 and PR0535, digested with KpnI and MluI and cloned in pTRE-Bi (Clontech# 631068)

PIR 3X HNF1A Cre-2A-PIT2 (pBA703): PCR amplify pNL108 with PR2967-PR2968 digest AgeI-BspQI and clone in pBA066 digested with the same enzymes.

PIR 3X C-C Cre-2A-PIT2 (pBA707): PCR amplify pNL108 with PR2967-PR2968 digest AgeI-BspQI and clone in pBA477 digested with the same enzymes.

PIR RE 1x TCF/LEF RE minTATA Cyan F4- 2A-PIT* (pBA790): pBA435 was digested with AscI and NdeI and ligated with annealed oligos (PR3094-PR3095) harboring matching overhangs. Using the same strategy we construct also:

PIR RE 3x TCF/LEF RE minTATA Cyan F4- 2A-PIT* (pBA791): Oligos PR3096-PR3097

PIR RE 6x TCF/LEF RE minTATA Cyan F4- 2A-PIT* (pBA791B): Oligos PR3098-PR3099

PIR RE 3x NFATC1 RE minTATA Cyan F4- 2A-PIT* (pBA612): pBA435 was digested with AscI and NdeI and ligated with annealed oligos (PR2465-PR2466) harboring matching overhangs. Using the same strategy we construct also:

PIR RE 1x NFATC1 RE minTATA Cyan F4- 2A-PIT* (pBA794): Oligos PR3104-PR3105

PIR RE 2x NFATC1 RE minTATA Cyan F4- 2A-PIT* (pBA795): Oligos PR3106-PR3107

PIR RE 1x HIF1 RE minTATA Cyan F4- 2A-PIT* (pBA826): pBA435 was digested with AscI and NdeI and ligated with annealed oligos (PR3217-PR3218) harboring matching overhangs. Using the same strategy we construct also:

PIR RE 2x HIF1 RE minTATA Cyan F4- 2A-PIT* (pBA827): Oligos PR3219-PR3220

PIR RE 3x HIF1 RE minTATA Cyan F4- 2A-PIT* (pBA828): Oligos PR3221-PR3222

PIR 1x TCF/LEF RE minTATA Cyan-F4-2A-PIT2 (pBA802): A HNF1 Feedback Loop backbone (pBA141) was digested with AscI and NdeI and ligated with annealed oligos (PR3094-PR3095) harboring matching overhangs. In this study we similarly construct and use:

PIR RE 3x TCF/LEF RE minTATA Cyan F4- 2A-PIT2 (pBA802): Oligos PR3096-PR3097

PIR RE 6x TCF/LEF RE minTATA Cyan F4- 2A-PIT2 (pBA803): Oligos PR3098-PR3099

PIR RE 3x NFATC1 RE minTATA Cyan F4- 2A-PIT2 (pBA612): A HNF1 Feedback Loop backbone (pBA141) was digested with AscI and NdeI and ligated with annealed oligos (PR2465-PR2466) harboring matching overhangs. Using the same strategy we construct also:

PIR RE 1x NFATC1 RE minTATA Cyan F4- 2A-PIT2 (pBA807): Oligos PR3104-PR3105

PIR RE 2x NFATC1 RE minTATA Cyan F4- 2A-PIT2 (pBA808): Oligos PR3106-PR3107

PIR RE 1x HIF1A RE minTATA Cyan F4- 2A-PIT2 (pBA820): A HNF1 Feedback Loop backbone (pBA141) was digested with AscI and NdeI and ligated with annealed oligos (PR3217-PR3218) harboring matching overhangs. Using the same strategy we construct also:

PIR RE 2x HIF1A RE minTATA Cyan F4- 2A-PIT2 (pBA821): Oligos PR3219-PR3220

PIR RE 3x HIF1A RE minTATA Cyan F4- 2A-PIT2 (pBA822): Oligos PR3221-PR3222

pTRE Bidirectional mCherry- CA-NFATC1 (pBA888B): CA-NFATC1 coding sequence was PCR amplified from Addegene Plasmid #11102 (CA-NFAT2) with primers PR3329-PR3330 digested with AgeI and PsPOMI and cloned in the pIM003 backbone digested using the same restriction sites.

Representative minimal promoters. We show here as an example the 3X sensors promoters. The PIR (PIT Response Element) is in red, the different transcription factor specific response elements are depicted in blue, the sequence of our minimal TATA is in green and the starting codon of the coding sequence (ATG) is in bold. The distance is counted starting from the center of the PIR (G in bold red) to the base preceding the TATAAT consensus (G in bold green).

PIT R.E. TF RE min minTATA **Start Codon**

3X HNF1A:

GAAATAGCGCTGTACAGCGTATGGGAATCTCTT**G**TACGGTGTACGAGTATCTTCCCGTACACCGTACGGCGCGCCAGTTAA
TAATTAACTAGTTAATAATTAACTAGTTAATAATTAACTCATATGCTCTAGAGG**G**TATATAATGGGGGCCACTAGTCTACT
ACCAGAGCTCATCGCTAGCGCTACCGGTCGCCACC**ATG**

3X HNF4A:

GAAATAGCGCTGTACAGCGTATGGGAATCTCTT**G**TACGGTGTACGAGTATCTTCCCGTACACCGTACGGCGCGCCGGTTCA
AAGTCCAGGTTCAAAGTCCAGGTTCAAAGTCCACATATGCTCTAGAGG**G**TATATAATGGGGGCCACTAGTCTACTACCAGA
GCTCATCGCTAGCGCTACCGGTCGCCACC**ATG**

3X C-C SOX10:

GAAATAGCGCTGTACAGCGTATGGGAATCTCTT**G**TACGGTGTACGAGTATCTTCCCGTACACCGTACGGCGCGCCCTACAC
AAAGCCCTCTTTGTGAGACTACACAAAGCCCTCTTTGTGAGACTACACAAAGCCCTCTTTGTGAGACATATGCTCTAGAGG
GTATATAATGGGGGCCACTAGTCTACTACCAGAGCTCATCGCTAGCGCTACCGGTCGCCACC**ATG**

3X HIF1A:

GAAATAGCGCTGTACAGCGTATGGGAATCTCTT**G**TACGGTGTACGAGTATCTTCCCGTACACCGTACGGCGCGCCGACCTT
GAGTACGTGCGTCTCTGCACGTATGGACCTTGAGTACGTGCGTCTCTGCACGTATGGACCTTGAGTACGTGCGTCTCTGCA
CGTATGCATATGCTCTAGAGGG**T**ATATAATGGGGGCCACTAGTCTACTACCAGAGCTCATCGCTAGCGCTACCGGTCGCCA
CC**ATG**

3X TCF/LEF:
GAAATAGCGCTGTACAGCGTATGGGAATCTCTT**G**TACGGTGTACGAGTATCTTCCCGTACACCGTACGGCGCGCCAGATCA
AAGGGGGTAAGATCAAAGGGGGTAAGATCAAAGGGGGTACATATGCTCTAGAGG**G**TATATAATGGGGGCCACTAGTCTACT
ACCAGAGCTCATCGCTAGCGCTACCGGTCGCCACC**ATG**

3X NFATC1:
GAAATAGCGCTGTACAGCGTATGGGAATCTCTT**G**TACGGTGTACGAGTATCTTCCCGTACACCGTACGGCGCGCCGGAGGA
AAAACTGTTTCATACAGAAGGCGTGGAGGAAAAACTGTTTCATACAGAAGGCGTGGAGGAAAAACTGTTTCATACAGAAGG
CGTCATATGCTCTAGAGG**G**TATATAATGGGGGCCACTAGTCTACTACCAGAGCTCATCGCTAGCGCTACCGGTCGCCACC**A**
TG

Cell culture and transfection procedure. The experiments in this work are performed on five different cell lines: HEK293 Tet-On Advanced, HEK293, HuH-7, HeLa and HCT-116. HEK293 Tet-On Advanced cell lines were originally purchased from Clontech (Cat # 630931) and HEK293 (293-H) cells were purchased from Invitrogen (Cat # 11631-017).

HCT-116 were purchased from the Deutsche Sammlung von Mikroorganismen und Zellkulturen (DSMZ) (cat. no. ACC581). Both HEK293 lines were cultured at 37 ºC, 5% CO_2 in RPMI-1640 medium (Gibco, Life Technologies; Cat # A10491-01), supplemented with 10% FBS (Sigma-Aldrich; Cat # F9665). Splitting was performed every 3-4 days using 0.25% Trypsin- EDTA (Gibco, Life technologies; Cat # 25200-072). HuH-7 cells were purchased from the Health Science Research Resources bank of the Japan Health Sciences Foundation (Cat-# JCRB0403, Lot-# 07152011) and cultured at 37 °C, 5% CO_2 in DMEM, low glucose, GlutaMAX (Life technologies, Cat #21885-025), supplemented with 10% FBS (Sigma-Aldrich, Cat #F9665 or Life technologies, Cat #10270106). HeLa cells were purchased from ATCC (Cat # CCL-2, Lot: 58930571) and cultured at 37°C, 5% CO_2 in DMEM, high glucose (Life technologies, Cat #41966), supplemented with 10% FBS (Sigma-Aldrich, Cat #F9665 or Life Technologies, Cat #10270106). All the media are supplemented with 1% Penicillin/Streptogamine Solution (Sigma-Aldrich, Cat #P4333). Cultures were propagated for at most two months before being replaced by fresh cell stock.

Transfections. All transfections were performed using Lipofectamine 2000 Transfection Reagent (Life Technologies) according to the suggested guidelines. All transfections used for data binning and fitting were performed in uncoated 6-well plates (Thermo Scientific Nunc) in order to collect a large number of single cell measurements. The cells were seeded 24 h before transfection at a density per well of 3.5 x 10^5 for HEK293 Tet-On and HEK293, 3x 10^5 for HeLa and 2.5x 10^5 for HuH-7 in order to have an 80-90% confluence at the time of transfection. The plasmids for each sample were mixed according to **Table S4** (see different tabs that refer to individual panels) and diluted into 250 μl of Opti-MEM I Reduced Serum (Gibco, Life technologies Cat # 31985-962). Lipofectamine 2000 was diluted in 250 μl Opti-MEM I per sample to a final amount of 2.5:1 ml Reagent/mg DNA ratio. After an incubation of 5 minutes the diluted Lipofectamine was added to the diluted DNA sample. The resulting mixture was briefly mixed by gentle vortexing and incubated 20 minutes at room temperature before being added to the cells. When required Doxycycline hyclate (Fluka, Cat # 44577) was added right after transfection starting from a 1000x stock to a 1000 ng/mL final concentration.

Microscopy. Microscopy images were taken 48 h after transfection. We used the Nikon Eclipse Ti microscope equipped with a mechanized stage and temperature control chamber held at 37 °C during the image acquisition. The excitation light was generated by a Nikon IntensiLight C-HGFI mercury lamp and filtered through a set of optimized Semrock filter cubes. The resulting images were collected by an Hammamatsu, ORCA R2 camera using a 10X objective. Each Semrock cube is assembled from an excitation filter, a dichroic mirror and an emission filter. In order to minimize the crosstalk between the different fluorescent proteins we used the following setup: **amCyan:** CFP HC (HC 438/24, BS 458, HC 483/32), **mCitrine**: YFP HC (HC 500/24, BS 520, HC 542/27), **mCherry:** TxRed HC (HC 624/40, BS 593, HC 562/40), **iRFP:** Cy5.5-A (HC 655/40, BS 685, HC 716/40). The images shown in Figure 6 were acquired with an exposure of 200 ms for AmCyan and 2 s for iRFP given the low sensitivity of CMOS sensors for the low energy part of the spectrum. The images in Figure 7 are recorded using an exposure of 200 ms for mCitrine, 800 ms for mCherry and keep the previous settings for AmCyan and iRFP. The acquired images were processed by ImageJ software performing uniform contrast-enhancement to improve visualization. All the images in each panel were treated with the same parameters.

Conversion factor between high and low PMT voltages for output measurements. To extend the measurement dynamic range for FACS measurements and cover with reasonable sensitivity values spanning several order of magnitudes, from the low expression levels of the uninduced open loop to the induced feedback loop response, we used two different PMT settings for Amcyan: 400V for the open loop measurements and 250V for the feedback loop measurements. To establish a conversion factor we measured the SPHERO RainBow Calibration particles at two different PMT and calculated the intensity ratio for each peak (**Figure S2A**). Since the particles are very uniform this method is extremely accurate. However, the beads emission in the Cyan channel is low compared to the levels reached by some of fluorescent constructs. Furthermore the amplification factor could be sensitive to the difference in the specific emission spectrum between the beads and AmCyan.

To validate the method we measured several samples containing AmCyan and iRFP at both PMTs for Cyan while keeping the iRFP PMT voltage constant between the two measurements. In this way the iRFP value can be used as a reference to relate two separate measurements. In particular the iRFP-Cyan data sets obtained in this way from both measurements were binned by similar iRFP values and a conversion factor for each pair was calculated by dividing the corresponding mean Cyan measured at PMT 400 by the one measured at PMT 250. All the generated data points were used to calculate a linear regression between the "conversion factors" and the iRFP levels (**Figure S2B**). The resulting linear fitting has a slight positive slope for increasing levels of cyan but can be approximated by a constant for an extended dynamic range. Ultimately, a constant factor of 28 was used for simplicity, since the exact value has very little effect on our data analysis.

Synergy Measurements Setup. In order to balance the DNA employed in the transfection, equalize transcriptional and translational load on cells and have comparable levels of mCherry when withholding the TF or the AA plasmids in Figure 3 experiments, we substitute it with an analogous inducible plasmid coding for mCherry and a balancing factor that does not trigger a response. This setup creates very similar experimental condition among the different states. To confirm that

the expression of balancing factors does not affect the observed synergy, we conducted a control experiment in which the transfection is balanced by plasmids expressing exclusively mCherry. We call this second configuration Unbalanced (**Figure S3F**). The synergistic behavior is conserved (**Figure S3G** left), and the measured synergy scores are not significantly affected by the absence of the balancing factor (**Figure S3G** right). To confirm that the synergy does not arise from interaction of the mutant PIT* protein with regulators, we remove PIT2* from the highest-synergy 3x HNF1A/B composite promoter so that it expresses the Cyan fluorescent reporter exclusively. The removal of PIT* does not result in a significant change in the observed synergy score (**Figure S3H**).

Distance definition in synergy measurements. All base pairs distances (bp) are calculated by counting from the center of the amplifier activator (AA) response element to the bp preceeding the TATA consensus sequence.

Synergy Score Calculation. Synergy is defined as the deviation from additive linear response and calculated as the ratio between the expression in the presence of both TF and AA, divided by the sum of expression with TF only and AA only. To yield more consistent results all the measurements in **Figure 3** are carried out at the same settings used for the feedback loop (PMT 250). Given the low expression level for TF only induction, the signal in these conditions is barely above background, reducing our ability to accurately discriminate differences between response element variants. To increase the precision of the calculation we use TF induction values derived from the measurements in **Figures 1 B-D** where we use high PMT and measure a large number of events. These measurements are then corrected for the factor of 5 introduced by the 2A element in the constructs used for synergy characterization (**Figure S3B**).

Forward engineered sensors measurements: HIF1A is induced by adding 250 μM of $COCl_2$ (Sigma C8661) 24h after transfection. (Li et al, 2006) TCF/LEF response is induced by adding 50 mM LiCl (Sigma 203637) 24h after transfection.(Li et al, 2006) NFATC1 activation is obtained through the ectopic expression of a NFATC1 calcium sensitive variant (pBA888B) successively induced by adding 10 ng/ml of PMA (Sigma P1585) and 0.5 mM of Ionomycin (Tocris 2092) 24h after transfection.(Boss et al, 1996) The cells were harvested and measured 48h after transfection resulting in a 24h stimulation time for all the chemical inducers.

AND gate measurements. The plasmid composition for the AND-gate characterization in Figure 6 are in **Table S4**. We note that balancing factors were used, similar to the procedure employed in synergy characterization.

Flow Cytometry. The cells were prepared for FACS analysis 48 h after transfection by removing the medium and incubating the cells with 300 ml phenol-red free Trypsin (0.5% Trypsin-EDTA (Gibco, Life Technologies, cat # 15400-054) at 37°C for 3 minutes (HEK293, HEK293 Tet-On) or 5-6 minutes (HuH-7 and HeLa). After incubation, the Trypsin concentration was diluted 1:2 with PBS (Gibco, Life Technologies cat # 10010-56) and the suspended cells were transferred to FACS tubes (Life Systems Design, Cat # 02-1412-000) and kept on ice. To avoid potential cell damage the samples were prepared in successive batches so that no single sample was kept on ice for more than 1 h. The prepared samples were measured using a BD LSR Fortessa II Cell Analyzer with a combination of excitation and emission that minimizes the crosstalk between different fluorescent reporters. AmCyan was measured with a 445 nm laser and a 473/10 nm emission filter, mCherry with a 561 nm excitation laser coupled to a 600 nm longpass filter and 610/20 emission filter, mCitrine with 488 nm laser, 505 nm longpass filter and 542/27 nm emission filter and iRFP using a 640 nm excitation laser and 710/50 emission filter. The iRFP transfection control was measured at PMT voltage of 300 in all the experiments, representing a constant baseline. Other PMT voltages were chosen to take the full advantage of the dynamic range, but were kept consistent in experiments that are directly compared. In particular, mCherry was measured using a PMT voltage of 300V in the TF induction experiments and 350 V when used as a target for downstream knockdown, but the two dataset are never compared. mCitrine is measured at 250 V. In order to extend the dynamic range, AmCyan is measured at 400 V in experiments with open loop sensor and at 250 V in experiments with feedback-amplified sensors, and at 300 V when the feedback loop is used to drive downstream repression. Several of the samples have been measured at different Cyan PMT voltages to build a conversion function and allow samples comparison across different PMT Values. SPHERO RainBow Calibration particles (Cat # 559123, BD) and Align Flow Cytometry beads (Cat # A16500, Life Technologies) were used to ensure constant device performance and to qualitatively validate the PMT conversion factors obtained for AmCyan.

Data Analysis. General flow cytometry data analysis for bar charts was performed using FlowJo software. In this work we use three different fluorescent units: absolute, relative and normalized. Absolute values (**abs. u.**) are the direct numerical values measured by the instrument; when feedback-amplified sensors are shown, these values are multiplied by the factor 28 to be comparable to open-loop sensors. These units are typically used to present binned data.

Relative expression units (**rel. u.**) are calculated as follows. (i) Live cells are gated based on their forward and side-scatter readouts. (ii) Within this gate, cells positive in a given fluorophore are gated based on a negative control such that 99.9% of cells in this single-color control sample fall outside of the selected gate. (iii) For each positive cell population in a

given channel, the mean value of the fluorescent intensity is calculated and multiplied by the frequency of the positive cells. This value is used as a measure for the total reporter signal in a sample and can be defined as Total Intensity (TI). The total intensity of a given output is normalized by the frequency of iRFP-positive cells (constitutive transfection control) to account for day-to-day variations in transfection efficiency or cell state. The procedure can be summarized in the following formula: Reporter intensity in rel. u. = [mean(Reporter in Reporter+ cells) * Frequency (Reporter+ cells)] / frequency (Transfection Marker+ cells). Relative units are used when we directly compare expression levels between different cell lines, since constitutive promoters of transfection control have very different strength in different cell lines and the use of normalized units (below) is inappropriate.

Normalized units (**norm. u**) are obtained by dividing the total intensity of the output of interest (as defined above) by the total intensity of the iRFP transfection control.
The relative formula is therefore: Reporter intensity in norm. u. = [mean(Reporter in Reporter+ cells) * Frequency (Reporter+ cells)] / [mean (Transfection Marker in Transfection Marker+ cells) * Frequency (Transfection Marker+ cells)]. Normalized units are a more robust indicator when the comparison is done between measurements taken from the same cell line.

The provided flow cytometry plot data are created through the FlowJo Layout editor and gated to show the same number of gated live cells (190000). The shown plots are selected as representative samples out of a biological triplicate.

Fine binning for the fitting. The flow cytometry data from a biological triplicate measurement containing in total 6-8 million cells for HEK293 Tet-On and 2-3 million cells with HuH-7, was exported without gating into csv format while pooling the triplicate data. The gating was performed in Matlab by a conservative oval gate on forward-side scatter plot to exclude dead cells and debris. All cells whose Cyan levels fell within a given bin were collected together and their value averaged. The bins were spaced at equal 1000 instrument units apart (with the entire range between -200 to 250000 units). Fitting was performed without weighting.

Modeling of open-loop binned data. The model of open loop induction with two genes reflecting the assay in HEK293 Tet-On cell was created using a system of differential equations. We model TF binding as a second-order process, resulting in an activation function with a Hill coefficient of 1, due to the lack of data that suggest otherwise. The explanation of the different terms is as follows:

$[HNF]$	Concentration of free HNF TF in a cell
$[G_{HNF}]$	Copy number of HNF-encoding gene in a cell
$[G_{Cyan}]$	Concentration of unbound sensor gene in a cell
$[G_{Cyan}::HNF]$	Concentration of the sensor gene bound to HNF factor in a cell
$[G_{Cyan}^{(0)}]$	Initial copy number of sensor gene in a cell
$[Cyan]$	Concentration of sensor output, AmCyan
$k_{syn}^{(1)}$	Lumped expression rate of HNF (DNAè Protein)
$k_{syn}^{(2)}$	Lumped expression rate of Cyan from TF-bound DNA complex (DNAè Protein)
k_{ON}^{HNF}	Association rate constant of HNF to its sensor
k_{OFF}^{HNF}	Dissociation rate of HNF from the bound complex
k_{DEG}^{HNF}	HNF degradation rate constant
k_{DEG}^{Cyan}	Cyan degradation rate constant

The mass-balance of the HNF transcription factor, expressed from the HNF-encoding gene G_{HNF}:

$$\frac{d[HNF]}{dt} = k_{syn}^{(1)}[G_{HNF}] - k_{ON}^{HNF}[G_{Cyan}][HNF] + k_{OFF}^{HNF}[G_{Cyan}::HNF] - k_{DEG}^{HNF}[HNF] \quad \text{(S.1)}$$

The mass-balance of HNF-bound sensor:

$$\frac{d[G_{Cyan}::HNF]}{dt} = k_{ON}^{HNF}[G_{Cyan}][HNF] - k_{OFF}^{HNF}[G_{Cyan}::HNF] \quad \text{(S.2)}$$

Mass-balance of Cyan:

$$\frac{d[Cyan]}{dt} = k_{syn}^{(2)}\left[G_{Cyan}::HNF\right] - k_{DEG}^{Cyan}[Cyan] \quad \text{(S.3)}$$

Mass-balance of bound and unbound sensor species:

$$[G_{Cyan}] = [G_{Cyan}^{(0)}] - \left[G_{Cyan}::HNF\right] \quad \text{(S.4)}$$

In the steady state, the analytical solution (Mathematica®) is as follows

$$[HNF] = k_{syn}^{(1)}\frac{G_{HNF}}{k_{DEG}^{HNF}} \quad \text{(S.5)}$$

$$[Cyan] = \frac{k_{syn}^{(2)}k_{ON}^{HNF}k_{syn}^{(1)}[G_{Cyan}^{(0)}][G_{HNF}]}{k_{DEG}^{Cyan}\left(k_{DEG}^{HNF}k_{OFF}^{HNF} + k_{ON}^{HNF}k_{syn}^{(1)}[G_{HNF}]\right)} \quad \text{(S.6)}$$

$$\left[G_{Cyan}::HNF\right] = \frac{k_{ON}^{HNF}k_{syn}^{(1)}[G_{Cyan}^{(0)}][G_{HNF}]}{k_{DEG}^{HNF}k_{OFF}^{HNF} + k_{ON}^{HNF}k_{syn}^{(1)}[G_{HNF}]} \quad \text{(S.7)}$$

We assume that in a co-transfection experiment,

$$[G_{Cyan}^{(0)}] = [G_{HNF}] = G$$

and then

$$[Cyan] = \frac{k_{syn}^{(2)}k_{ON}^{HNF}k_{syn}^{(1)}G^2}{k_{DEG}^{Cyan}\left(k_{DEG}^{HNF}k_{OFF}^{HNF} + k_{ON}^{HNF}k_{syn}^{(1)}G\right)} \quad \text{(S.8)}$$

This functional form can be fitted to the data obtained in measurements. The actual form used for fitting is

$$[AmCyan] = \frac{[mCherry]^2}{b_1 + b_2[mCherry]} + b_3 \quad \text{(S.9)}$$

Where

$$[mCherry] = \alpha[G]$$

(The linear relationship between the gene copy number and fluorescence was established in earlier work (Bleris et al, 2011))

Modeling of synergistic feedback amplification and simulations

The model was built in SimBiology Matlab toolbox (**Figure S4E**). In this model regulator binding is modeled as a second-order process, resulting in an activation function with a Hill coefficient of 1, due to the lack of data that suggest otherwise. The concentration is measured in "molecules", which means "molecules per mammalian cell" such that 1 "molecule" = 10^{-12} M (assuming cell volume of 1660 μm^3). The main processes and parameters are summarized below:

1. Expression of mCherry and ectopic TF from a DNA cassette. The cassette copy number is set to 10 to represent a mean copy number in a transent transfection. The processes are modeled as separate transcription and translation, with both mRNA and protein degraded in first-order processes. Transcription rate is 0.003 1/s and translation rate is 0.008 1/s. RNA degradation rate is $6*10^{-5}$ 1/s corresponding to half-life about about 3 hours, and protein degradation rate is $8.02*10^{-6}$ 1/s

for mCherry, corresponding to half-life of 24 hours (stable protein); and $1.6*10^{-5}$ 1/s for the TF, corresponding to half life of 12 hours.

2. Binding of activators to sensor DNA. Sensor DNA exists in four configurations: naked DNA; DNA complexed to a transcriptional input (DNA::TF); DNA complexed to an amplifier activator (DNA::AA) and DNA complexed to both (DNA::TF::AA). Spieces can interconvert through binding and unbinding of proteins. Unbinding of all proteins has a rate constant of 0.01 1/sec. Binding of proteins is as follows: TF binding rate constant ranges between 10^{-8} ... 10^{-5} $s^{-1}molecule^{-1}$. Binding rate constant of AA: 10^{-8} ... 10^{-5} $s^{-1}molecule^{-1}$. To avoid accumulation of bound species, they are also converting back to naked DNA with the rate that equals the general protein degradation rate of $1.6*10^{-5}$ 1/s.

3. Expression of output and amplifier activator (in the case of feedback). The three bound complexes can express RNA coding for an output and an amplifier activator. The expression rate from DNA::TF complex is set at $6*10^{-5}$ 1/s and from a DNA:TF::AA complex at 0.003 1/s (50 times higher). The expression from DNA::AA complex is set either at 0.003 1/s for lack of synergy, or at a lower number, corresponding to synergy factor. In most simulations it is set at $6*10^{-5}$ 1/s. There is a splicing step to desicribe the splicing of miR-FF4 (rate of 0.01 1/s) and the resulting mRNA is translated into AmCyan with the rate of 0.008 1/s and, in the case of positive feedback, also to AA with the same rate. To model the lack of feedback, this reaction rate is set to zero.

Figure 4E, Figure S4F: The binding rate constants of activators (TF and AA) were scanned in 10-fold increases from 10^{-8} to 10^{-5} $s^{-1}molecule^{-1}$. For each assignment of the binding rate constants, the expression rate of the TF was varied as indicated on the X axis. For the open-loop output simulation, the translation of AA was set to zero. For closed-loop, it was set to 0.008 1/s. For feedback without synergy, the expression rates for different complexes were as follows: DNA::TF: $6*10^{-5}$ 1/s; DNA::AA: 0.003 1/s; DNA::TF::AA: 0.003 1/s. For a feedback with synergy, as follows: DNA::TF: $6*10^{-5}$ 1/s; DNA::AA: $6*10^{-5}$ 1/s; DNA::TF::AA: 0.003 1/s.

Figure 4G: The expression rate settings to reflect the presence and the absence of synergy are the same as in **Figure 4E**. The binding rate constant of AA was set to 10^{-6} $s^{-1}molecule^{-1}$. The binding rate constant of the TF was scanned between 10^{-8} ... 10^{-5} $s^{-1}molecule^{-1}$ as plotted on the X axis.

Figure 4J: The binding rate constants of activators were set to 10^{-6} $s^{-1}molecule^{-1}$. The expression rates were set as follows: DNA::TF: $3*10^{-5}$ 1/s; DNA::AA: 0.003/[synergy] 1/s; DNA::TF::AA: 0.003 1/s. Synergy was varied between 1 and 100. For each synergy value, the "off" output was simulated by setting the expression rate of TF to $3*10^{-6}$ 1/s (representing low leakage) and the "on" level was simulated by setting the expression rate of TF to $3*10^{-3}$ 1/s. The On, Off and the On:Off values are plotted.

Supplemental References

Bleris L, Xie Z, Glass D, Adadey A, Sontag E, Benenson Y (2011) Synthetic incoherent feedforward circuits show adaptation to the amount of their genetic template. *Molecular Systems Biology* **7**

Boss V, Talpade DJ, Murphy TJ (1996) Induction of NFAT-mediated transcription by Gq-coupled receptors in lymphoid and non-lymphoid cells. *The Journal of biological chemistry* **271:** 10429-10432

Buckley SMK, Delhove JMKM, Perocheau DP, Karda R, Rahim AA, Howe SJ, Ward NJ, Birrell MA, Belvisi MG, Arbuthnot P, Johnson MR, Waddington SN, McKay TR (2015) In vivo bioimaging with tissue-specific transcription factor activated luciferase reporters. *Sci Rep-Uk* **5**

Chen Z, Manley JL (2003) Core promoter elements and TAFs contribute to the diversity of transcriptional activation in vertebrates. *Molecular and cellular biology* **23:** 7350-7362

Fang B, Mane-Padros D, Bolotin E, Jiang T, Sladek FM (2012) Identification of a binding motif specific to HNF4 by comparative analysis of multiple nuclear receptors. *Nucleic Acids Research* **40:** 5343-5356

Fiering S, Northrop JP, Nolan GP, Mattila PS, Crabtree GR, Herzenberg LA (1990) Single Cell Assay of a Transcription Factor Reveals a Threshold in Transcription Activated by Signals Emanating from the T-Cell Antigen Receptor. *Gene Dev* **4:** 1823-1834

Huang Q, Gong C, Li J, Zhuo Z, Chen Y, Wang J, Hua ZC (2012) Distance and helical phase dependence of synergistic transcription activation in cis-regulatory module. *PloS one* **7:** e31198

Kuhlbrodt K, Herbarth B, Sock E, Hermans-Borgmeyer I, Wegner M (1998) Sox10, a novel transcriptional modulator in glial cells. *The Journal of neuroscience : the official journal of the Society for Neuroscience* **18:** 237-250

Lagrange T, Kapanidis AN, Tang H, Reinberg D, Ebright RH (1998) New core promoter element in RNA polymerase II-dependent transcription: sequence-specific DNA binding by transcription factor IIB. *Genes & development* **12:** 34-44

Lapique N, Benenson Y (2014) Digital switching in a biosensor circuit via programmable timing of gene availability. *Nature Chemical Biology* **10:** 1020-1027

Larsson E, Lindahl P, Mostad P (2007) HeliCis: a DNA motif discovery tool for colocalized motif pairs with periodic spacing. *BMC bioinformatics* **8:** 418

Leisner M, Bleris L, Lohmueller J, Xie Z, Benenson Y (2010) Rationally designed logic integration of regulatory signals in mammalian cells. *Nature Nanotechnology* **5:** 666-670

Li QF, Wang XR, Yang YW, Lin H (2006) Hypoxia upregulates hypoxia inducible factor (HIF)-3alpha expression in lung epithelial cells: characterization and comparison with HIF-1alpha. *Cell research* **16:** 548-558

Peirano RI, Wegner M (2000) The glial transcription factor Sox10 binds to DNA both as monomer and dimer with different functional consequences. *Nucleic Acids Res* **28:** 3047-3055

Prochazka L, Angelici B, Haefliger B, Benenson Y (2014) Highly modular bow-tie gene circuits with programmable dynamic behaviour. *Nature communications* **5**

Schodel J, Oikonomopoulos S, Ragoussis J, Pugh CW, Ratcliffe PJ, Mole DR (2011) High-resolution genome-wide mapping of HIF-binding sites by ChIP-seq. *Blood* **117:** E207-E217

Senkel S, Lucas B, Klein-Hitpass L, Ryffel GU (2005) Identification of target genes of the transcription factor HNF1beta and HNF1alpha in a human embryonic kidney cell line. *Biochimica et biophysica acta* **1731:** 179-190

Takagi H, King GL, Ferrara N, Aiello LP (1996) Hypoxia regulates vascular endothelial growth factor receptor KDR/Flk gene expression through adenosine A(2) receptors in retinal capillary endothelial cells. *Invest Ophth Vis Sci* **37:** 1311-1321

Takagi S, Nakajima M, Kida K, Yamaura Y, Fukami T, Yokoi T (2010) MicroRNAs regulate human hepatocyte nuclear factor 4alpha, modulating the expression of metabolic enzymes and cell cycle. *The Journal of biological chemistry* **285:** 4415-4422

Tronche F, Ringeisen F, Blumenfeld M, Yaniv M, Pontoglio M (1997a) Analysis of the distribution of binding sites for a tissue-specific transcription factor in the vertebrate genome. *Journal of molecular biology* **266:** 231-245

Tronche F, Ringeisen F, Blumenfeld M, Yaniv M, Pontoglio M (1997b) Analysis of the distribution of binding sites for a tissue-specific transcription factor in the vertebrate genome. *Journal of Molecular Biology* **266:** 231-245

Veeman MT, Slusarski DC, Kaykas A, Louie SH, Moon RT (2003) Zebrafish prickle, a modulator of noncanonical Wnt/Fz signaling, regulates gastrulation movements. *Curr Biol* **13:** 680-685

Weber W, Kramer BP, Fux C, Keller B, Fussenegger M (2002) Novel promoter/transactivator configurations for macrolide- and streptogramin-responsive transgene expression in mammalian cells. *The journal of gene medicine* **4:** 676-686

Wolner BS, Gralla JD (2000) Roles for non-TATA core promoter sequences in transcription and factor binding. *Molecular and cellular biology* **20:** 3608-3615

Wu G, Bohn S, Ryffel GU (2004) The HNF1beta transcription factor has several domains involved in nephrogenesis and partially rescues Pax8/lim1-induced kidney malformations. *European journal of biochemistry / FEBS* **271:** 3715-3728